

Received September 21, 2020, accepted October 5, 2020, date of publication October 8, 2020, date of current version October 20, 2020.

Digital Object Identifier 10.1109/ACCESS.2020.3029522

Adaptive Fault-Tolerant Guaranteed Performance Control for Euler-Lagrange Systems With Its Application to a 2-Link Robotic Manipulator

GANG ZHANG^{1,2,3} AND DEQIANG CHENG¹

¹School of Information and Control Engineering, China University of Mining and Technology, Xuzhou 221116, China

²Institute of Building Intelligence, Jiangsu Vocational Institute of Architectural Technology, Xuzhou 221116, China

³Jiangsu Collaborative Innovation Center for Building Energy Saving and Construction Technology, Xuzhou 221116, China

Corresponding author: Deqiang Cheng (cdqcumt@126.com)

This work was supported in part by the National Natural Science Foundation of China under Grant 51774281, in part by the National Key Research and Development Plan under Grant 2018YFC0808302, in part by the Technical Projects of Jiangsu Construction System under Grant 2017ZD006, in part by the Doctor Fund of Jiangsu Collaborative Innovation Center for Building Energy Saving and Construction Technology under Grant SJXTBS1702, and in part by the Scientific Project of Xuzhou under Grant KH17001.

ABSTRACT This paper investigates a novel adaptive fault-tolerant guaranteed performance control problem for Euler-Lagrange systems subject to unknown actuator faults. Firstly, a barrier Lyapunov function instead of logarithmic transformation is constructed to handle the performance constraints imposed on the controlled system. Then, an adaptive control scheme is devised to guarantee the prescribed tracking performance with consideration of the unknown actuator faults. Compared with the existing works, the prominent advantage of the proposed control method is that the detailed actuator fault information is not required to identify online and the complex logarithmic transformation is avoided. In this sense, the complexity of the developed controller is decreased dramatically, which is easily achievable in practice. Finally, application to a 2-link robotic manipulator is organized to validate the effectiveness of the proposed control method.

INDEX TERMS Euler-Lagrange system, prescribed performance control, robotic manipulator, adaptive fault-tolerant control.

I. INTRODUCTION

In recent years, adaptive control on nonlinear Euler-Lagrange (EL) systems has attracted considerable attention owing to the fact that EL systems can be used to describe various practical engineering systems such as robotic system, helicopter system and satellite system [1]–[6]. For example, a predictor-based tracking controller is developed for a EL system subject to time-delayed actuation, parameter uncertainty, and external disturbances in [7]. A stable control method is proposed to realize the trajectory tracking control for a planar three-link underactuated mechanical system with consideration of the gravity constraints in [8]. A robust autopilot controller is designed for a generic missile without consideration of the actuator nonlinearities, angle of attack constraint, and mismatched uncertainties by applying the barrier Lyapunov function and dynamic surface control techniques in [9]. As for the cooperative control of the multiple EL systems,

a distributed output tracking control scheme is devised for a class of EL multiagent systems with only using the measurable position information in [10]. To solve the actuator saturation problem, a dynamic auxiliary system is introduced for each EL agent system to obtain some auxiliary variables. And then a formation-containment control scheme is designed for the networked EL systems based on the auxiliary variables in [11].

However, in practice engineering, precise system information is difficult to obtain owing to the complex structure of the controlled object. In this case, unknown nonlinearity is often encountered in the corresponding controller design. In the existing works, neural network (NN) and fuzzy logic system as two effective tools have been widely utilized to approximate the unknown nonlinearities due to their superior approximation capability. For example, an adaptive tracking controller is devised for multiple uncertain EL systems via using a NN to approximate the unknown nonlinear functions in [12]. A two-layer NN-based adaptive distributed formation-containment control method is developed for

The associate editor coordinating the review of this manuscript and approving it for publication was Haibin Sun .

multiple EL systems via only using the output feedback information. Similar with NN-based adaptive control methods, adaptive fuzzy ones also have attracted wide attention. A fuzzy logic system is used to approximate the robot dynamics. And an adaptive control scheme is proposed based on the fuzzy approximation in [13]. Fuzzy approximation and backstepping techniques are integrated to develop an adaptive fuzzy optimal controller for the strict-feedback single-input and single-output nonlinear system in the presence of unmeasurable states and unknown nonlinear dynamics in [14]. Owing to its effectiveness and excellent control performance, the control method in [14] was extended to solve the output tracking problem for a group of strict-feedback nonlinear large-scale systems in [15]. Moreover, trajectory tracking control problem for multiple quad-rotor UAVs is solved by designing an adaptive fuzzy control scheme in [16]. Although effective, the relevant adaptive schemes based on the NN and fuzzy logic system are only valid in the relevant compact set. How to guarantee the adaptive scheme to keep on the compact set is pretty challenging both in theory and application [17]. Thus, it requires more efforts to conduct some further investigations on the adaptive control for EL systems.

In practice, actuator faults are often encountered, which will degrade the control performance or even lead to the system instability. A comprehensive survey of the fault diagnosis and fault-tolerant techniques is presented from the view of model-based and signal-based ways in [18], [19]. A low-complexity fault-tolerant control problem is investigated for multiple uncertain large-scale systems subject to unknown dead-zone input in [20]. An adaptive fuzzy fault-tolerant control scheme was proposed for a switched resistance-inductance-capacitance circuit system by applying the fuzzy-logic system to approximate the unknown internal dynamics in the presence of process fault. Wherein, a barrier Lyapunov function was constructed to make the system output be trapped into its constrained interval in [21]. Moreover, the recent development of spacecraft attitude fault-tolerant control methods are reviewed and analyzed in [22]–[24]. Faced with the actuator faults, how to guarantee the tracking performance of the controlled system is very challenging. To solve this problem, Bechlioulis and Rovithakis proposed a brand-new control method, named as prescribed performance control (PPC), to quantitatively characterize the transient and steady-state performance of the controlled system in 2008 [25]. Due to its prominent advantage in the control performance synthesis, PPC has attracted considerable attention in the existing works [26], [27]. For example, a NN-based adaptive PPC scheme is formulated for uncertain nonlinear systems in [28]. The constrained PPC problem is investigated for uncertain EL systems with consideration of full-state constraints in [29]. Moreover, to solve the control saturation, a bounded-input PPC scheme is developed for uncertain EL system in [30]. To enhance the robustness of the PPC method, an adaptive sliding mode disturbance observer-based composite control scheme is devised for space manipulators

in [31]. Although effective, the usage of logarithmic transformation in the PPC structure makes it very complex in the relevant controller design. Meanwhile, the logarithmic transformation is very sensitive to uncertainties and external disturbance. As an alternative, barrier Lyapunov function is a potential tool to deal with the state performance constraints existed in the traditional PPC method. For example, an output tracking constrained control protocol was investigated for switched uncertain nonlinear systems with consideration of unknown dead-zone nonlinearity by combining a time-varying tan-type barrier Lyapunov function and fuzzy logic system in [32]. Moreover, an integral barrier Lyapunov function was proposed to derive a full-state constrained adaptive control scheme for a class of uncertain switched nonlinear system in [33]. Although effective, the application of fuzzy logic systems in the above reference works makes it pretty challenging and complex to tune the relevant adaptive parameters online. Thus, how to conquer the above limitations deserve further investigations.

In this paper, a novel adaptive guaranteed performance control method is proposed for EL system with unknown actuator faults. Compared with the existing works, the prominent contributions of this work are twofold:

- i. The detailed information of the unknown actuator faults is not required to identify online. This decreases the complexity of the relevant control system design dramatically.
- ii. The complex logarithmic transformation in the conventional PPC structure is omitted, which makes the relevant controller scheme easily achievable in practice. Meanwhile, norm inequality is applied to deal with the unknown nonlinear dynamics without using any neural or fuzzy approximation technique, which makes the tuning procedure for the relevant adaptive parameters much easier.

The rest of this paper is organized as follows. Section II gives the description of the EL system and actuator faults. The detailed procedure of the adaptive fault-tolerant control method is shown in Section III. Section IV shows the applications of the proposed control method to a 2-link robotic manipulator. Some detailed discussions and conclusions are drawn in Section V.

A. NOTATIONS

T , $\|\cdot\|$, $|\cdot|$ represent the vector transpose, the Euclidean norm of a vector, and the absolute value of a real number. \mathbb{R}^n , \mathbb{R}^{n+} are, respectively, the sets of n -dimensional real numbers and n -dimensional positive real numbers. $\sigma(\cdot)$ is the eigenvalue of a nonsingular matrix, respectively. \mathbb{N} , \mathbb{N}^+ denote the set of nonnegative integers and positive integers, respectively. For any two positive real numbers $\hat{q}_1, \hat{q}_2 \in \mathbb{R}^+$, if the two numbers satisfy $\hat{q}_1 > 1$, $\hat{q}_2 > 1$ and $\frac{1}{\hat{q}_1} + \frac{1}{\hat{q}_2} = 1$, then for any two positive variables $a, b \in \mathbb{R}^+$, the following inequality holds $a \cdot b \leq \frac{a^{\hat{q}_1}}{\hat{q}_1} + \frac{b^{\hat{q}_2}}{\hat{q}_2}$. When and only when

$a^{\hat{e}1} = b^{\hat{e}2}$, the ‘=’ can be obtained. This is the Young’s inequality based on [34].

II. SYSTEM DESCRIPTION AND ANALYSIS OF ACUTATOR FAULTS

A. DESCRIPTION OF EULER-LAGRANGE SYSTEM

In this paper, EL system, as a typical multiple-input-multiple-output one, is considered with the following universal form:

$$\mathbf{M}(\mathbf{p})\ddot{\mathbf{p}} + \mathbf{C}(\mathbf{p}, \dot{\mathbf{p}})\dot{\mathbf{p}} + \mathbf{G}(\mathbf{p}) = \mathbf{u} \quad (1)$$

where $\mathbf{p} = [p_1, \dots, p_n]^T \in \mathbb{R}^n$ is the general position vector of the EL system with n dimension. $\dot{\mathbf{p}}, \ddot{\mathbf{p}}$ are the relevant general velocity and accelerated velocity vectors, respectively. $\mathbf{M}(\mathbf{p}) \in \mathbb{R}^{n \times n}$, $\mathbf{C}(\mathbf{p}, \dot{\mathbf{p}}) \in \mathbb{R}^{n \times n}$, $\mathbf{G}(\mathbf{p}) \in \mathbb{R}^n$ denote, respectively, the general inertial matrix, the vector of Coriolis and Centrifugal torques, and the vector of gravitational torque, which are difficult to obtain precisely in practice. $\mathbf{u} \in \mathbb{R}^n$ represents the control torque of the EL system. For the EL system in (1), according to [35], there are four common properties listed as follows.

Property 1: Matrix $\dot{\mathbf{M}}(\mathbf{p}) - 2\mathbf{C}(\mathbf{p}, \dot{\mathbf{p}})$ is skew-symmetric, i.e.; $\mathbf{q}^T (\dot{\mathbf{M}}(\mathbf{p}) - 2\mathbf{C}(\mathbf{p}, \dot{\mathbf{p}})) \mathbf{q} = 0, \forall \mathbf{q} \in \mathbb{R}^n$.

Property 2: Matrix $\mathbf{M}(\mathbf{p})$ is positive-definite and symmetric. And there exist two positive constants $\underline{m} < \bar{m} \in \mathbb{R}$ having the following inequality hold: $0 < \underline{m}\mathbf{I}_n \leq \mathbf{M}(\mathbf{p}) \leq \bar{m}\mathbf{I}_n$.

Property 3: Vector of Coriolis and Centrifugal torques $\mathbf{C}(\mathbf{p}, \dot{\mathbf{p}})$ are continuous with respect to states $\mathbf{p}, \dot{\mathbf{p}}$. And there exists a positive constant \bar{c} making the inequality hold: $\|\mathbf{C}(\mathbf{p}, \dot{\mathbf{p}})\| \leq \bar{c} \|\dot{\mathbf{p}}\|$.

Property 4: Vector of gravitational torque $\mathbf{G}(\mathbf{p})$ is bounded, i.e.; there exists a positive constant \bar{g} making the following inequality hold $\|\mathbf{G}(\mathbf{p})\| \leq \bar{g}$.

Remark 1: The above four properties are very common in practical systems such as robotic manipulators and spacecraft attitude system. These properties are very beneficial to facilitate the subsequent controller design.

B. ANALYSIS OF ACTUATOR FAULTS

In practice, actuator failure is often encountered, which will degrade the control performance or even bring a serious threat for the system safety. Thus, it is of necessity to analyze the common actuator faults. In this work, multiplicative and additive actuator failures are considered, which can be modelled as:

$$\mathbf{u}_{actual}(t) = \mathbf{B}(t)\mathbf{u}(t) + \mathbf{u}_b(t) \quad (2)$$

where $\mathbf{B}(t) = \text{diag}\{B_1(t), \dots, B_n(t)\} \in \mathbb{R}^{n \times n}$ denotes the remaining control rate for multiplicative actuator fault, which is often unknown but its element satisfies $0 < \underline{b} \leq B_i(t) \leq 1$ with \underline{b} being a known constant. $\mathbf{u}_b(t)$ is an unknown additive actuator fault. Based on (2), system (1) becomes

$$\mathbf{M}(\mathbf{p})\ddot{\mathbf{p}} + \mathbf{C}(\mathbf{p}, \dot{\mathbf{p}})\dot{\mathbf{p}} + \mathbf{G}(\mathbf{p}) = \mathbf{B}(t)\mathbf{u}(t) + \mathbf{u}_b(t) \quad (3)$$

Remark 2: As shown in Eq. (3), it is easy to find that the external disturbance or noise in the control input can be

integrated into the additive actuator fault term $\mathbf{u}_b(t)$. In general, additive actuator fault refers to those unknown fault model and external disturbance or noise. Thus, to be brief, in this work, the additive actuator fault term $\mathbf{u}_b(t)$ contains the matched external disturbance or noise in the control input.

According to the foregoing analysis, the control objective of this work is twofold:

- i. The desired reference command \mathbf{p}_d can be tracked stably by the devised controller. And the prescribed transient and steady-state performance of the tracking error system can be guaranteed.
- ii. All the involved close-loop signals are uniformly ultimately bounded under the devised controller.

Before moving, there are two assumptions are imposed on the controlled EL system.

Assumption 1:-General position and velocity vectors $\mathbf{p}, \dot{\mathbf{p}}$ are available for measurement.

Assumption 2:-The desired reference command \mathbf{p}_d is continuous and its first derivative known.

Remark 3: In practice systems, position and velocity information is easily obtained by the measurement devices like laser radar. Thus, *Assumption 1* is reasonable. For *Assumption 2*, the desired reference command can be preplanned by the designers, i.e., it can be designed sufficiently smoothly. Thus, *Assumption 2* is also reasonable.

III. ADAPTIVE FAULT-TOLERANT GUARANTEED PERFORMANCE CONTROL METHOD

According to the foregoing discussions, a brand-new adaptive fault-tolerant guaranteed performance control method is investigated in this part. Before moving, the tracking error is defined as $\mathbf{p}_e = [p_{e,1}, \dots, p_{e,n}]^T = \mathbf{p} - \mathbf{p}_d$.

A. ADAPTIVE FAULT-TOLERANT GUARANTEED PERFORMANCE CONTROLLER DESIGN

To guarantee the tracking performance, the following performance constraint is imposed:

$$-\alpha_i(t) < p_{e,i}(t) < \alpha_i(t) \quad (4)$$

where $\alpha_i(t) > 0$ is the designed performance function. Without loss of generality, an exponential performance function is formulated, namely, it is:

$$\alpha_i(t) = (\alpha_{i,0} - \alpha_{i,\infty}) \exp(-\gamma_i t) + \alpha_{i,\infty} \quad (5)$$

where $\alpha_{i,0} \in \mathbb{R}$ is the initial state of $\alpha_i(t)$, which is positive. $\alpha_{i,\infty} > 0$ is the ultimate state of $\alpha_i(t)$. γ_i denotes the convergence rate of the performance function. To guarantee the tracking performance in the whole time domain, the value of $\alpha_{i,0}$ should satisfy $\alpha_{i,0} > |p_{e,i}(0)|$ ($i = 1, \dots, n$).

Remark 4: In Eq. (5), the parameters of performance function $\alpha_i(t)$ will affect the control performance of the Euler-Lagrange systems. As for the convergence rate γ_i , the larger the γ_i is, the faster the convergence of the tracking error system is. However, it will require a very large control input to support the fast convergence rate. So in practical

systems, the value of parameter γ_i can be set according to control ability of the actuator. As for the ultimate boundedness parameter $\alpha_{i,\infty}$, it represents the tracking accuracy. So it can be set according to the desired control requirement from the practical tasks. As for the rest parameters, they can be set freely when the foregoing basic conditions are satisfied.

As presented in (5), the tracking error $p_{e,i}$ ($i = 1, \dots, n$) will converge to a small set involved in the interval $(-\alpha_{i,\infty}, \alpha_{i,\infty})$ with an exponential velocity. To facilitate the subsequent controller design, the following standard tracking error is defined:

$$-1 < p_{e,i}(t)/\alpha_i(t) < 1 \quad (6)$$

To be brief, a newly defined state $\mathbf{x}_1 = [x_{1,1}, \dots, x_{1,n}]^T \in \mathbb{R}^n$ is given with its every element is

$$x_{1,i}(t) = p_{e,i}(t)/\alpha_i(t) \quad (7)$$

Backstepping technique, as an effective one, has been widely used to develop the relevant controller for the cascaded system [36]. So in this work, backstepping technique is applied to develop the relevant controller. In detail, there are two steps as follows.

*Step 1:-*Construct the following barrier Lyapunov function:

$$V_1 = \frac{1}{2} \sum_{i=1}^n \frac{x_{1,i}^2}{1-x_{1,i}^2} \quad (8)$$

Taking the derivative of V_1 yields

$$\begin{aligned} \dot{V}_1 &= \frac{1}{2} \sum_{i=1}^n \frac{2x_{1,i}(1-x_{1,i}^2) + 2x_{1,i}^3}{(1-x_{1,i}^2)^2} \dot{x}_{1,i} \\ &= \sum_{i=1}^n \frac{x_{1,i}}{(1-x_{1,i}^2)^2} \dot{x}_{1,i} \end{aligned} \quad (9)$$

Substituting (7) into (9) gets

$$\begin{aligned} \dot{V}_1 &= \sum_{i=1}^n \frac{x_{1,i}}{(1-x_{1,i}^2)^2} \left(\frac{\dot{p}_{e,i}\alpha_i - p_{e,i}\dot{\alpha}_i}{\alpha_i^2} \right) \\ &= \sum_{i=1}^n \frac{x_{1,i}}{(1-x_{1,i}^2)^2 \alpha_i} \left(\dot{p}_{e,i} - \frac{\dot{\alpha}_i}{\alpha_i} p_{e,i} \right) \end{aligned} \quad (10)$$

Due to $p_{e,i} = p_i - p_{d,i}$, (10) becomes

$$\dot{V}_1 \sum_{i=1}^n \frac{x_{1,i}}{(1-x_{1,i}^2)^2 \alpha_i} \left(\dot{p}_i - \dot{p}_{d,i} - \frac{\dot{\alpha}_i}{\alpha_i} p_{e,i} \right) \quad (11)$$

Based on the foregoing design procedure, we continue to define the following coordinate transformation:

$$\mathbf{x}_2(t) = \dot{\mathbf{p}}(t) - \mathbf{v}(t) \quad (12)$$

where $\mathbf{x}_2(t) = [x_{2,1}(t), \dots, x_{2,n}(t)]^T \in \mathbb{R}^n$ is the newly state vector under the coordinate transformation.

$\mathbf{v}(t) = [v_1(t), \dots, v_n(t)]^T \in \mathbb{R}^n$ is the first virtual controller to be determined later. Based on (12), (11) becomes

$$\dot{V}_1 = \sum_{i=1}^n \frac{x_{1,i}}{(1-x_{1,i}^2)^2 \alpha_i} \left(x_{2,i} + v_i - \dot{p}_{d,i} - \frac{\dot{\alpha}_i}{\alpha_i} p_{e,i} \right) \quad (13)$$

By applying Young's inequality, one can obtain

$$\frac{x_{1,i}}{(1-x_{1,i}^2)^2 \alpha_i} x_{2,i} \leq \frac{2x_{1,i}^2}{(1-x_{1,i}^2)^4 \alpha_i^2} + \frac{1}{4} x_{2,i}^2 \quad (14)$$

Based on (13) and (14), the virtual controller $v_i(t)$ is devised as

$$v_i = -K_{1,i} p_{e,i} + \dot{p}_{d,i} + \frac{\dot{\alpha}_i}{\alpha_i} p_{e,i} - \frac{2x_{1,i}}{(1-x_{1,i}^2)^2 \alpha_i} \quad (15)$$

where $\mathbf{K}_1 = \text{diag}\{K_{1,1}, \dots, K_{1,n}\} \in \mathbb{R}^{n \times n}$ is the positive-definite control gain matrix. Accordingly, substituting (15) into (13) yields

$$\dot{V}_1 \leq - \sum_{i=1}^n \frac{K_{1,i} x_{1,i}^2}{(1-x_{1,i}^2)^2} + \frac{1}{4} \sum_{i=1}^n x_{2,i}^2 \quad (16)$$

*Step 2:-*To design the true control input, the following Lyapunov function is devised

$$V_2 = V_1 + \frac{1}{2} \mathbf{x}_2^T \mathbf{M}(\mathbf{p}) \mathbf{x}_2 \quad (17)$$

Taking the derivative of V_2 yields

$$\begin{aligned} \dot{V}_2 &= \dot{V}_1 + \frac{1}{2} \mathbf{x}_2^T \dot{\mathbf{M}}(\mathbf{p}) \mathbf{x}_2 + \mathbf{x}_2^T \mathbf{M}(\mathbf{p}) \dot{\mathbf{x}}_2 \\ &= \dot{V}_1 + \frac{1}{2} \mathbf{x}_2^T \dot{\mathbf{M}}(\mathbf{p}) \mathbf{x}_2 + \mathbf{x}_2^T \mathbf{M}(\mathbf{p}) \ddot{\mathbf{p}} - \mathbf{x}_2^T \mathbf{M}(\mathbf{p}) \dot{\mathbf{v}} \end{aligned} \quad (18)$$

Substituting (3) into (18) gets

$$\begin{aligned} \dot{V}_2 &= \dot{V}_1 + \frac{1}{2} \mathbf{x}_2^T \dot{\mathbf{M}}(\mathbf{p}) \mathbf{x}_2 + \mathbf{x}_2^T (\mathbf{B}(t) \mathbf{u} + \mathbf{u}_b \\ &\quad - \mathbf{C}(\mathbf{p}, \dot{\mathbf{p}}) \dot{\mathbf{p}} - \mathbf{G}(\mathbf{p}) - \mathbf{M}(\mathbf{p}) \dot{\mathbf{v}}) \end{aligned} \quad (19)$$

Based on (12), (19) becomes

$$\begin{aligned} \dot{V}_2 &= \dot{V}_1 + \frac{1}{2} \mathbf{x}_2^T \dot{\mathbf{M}}(\mathbf{p}) \mathbf{x}_2 + \mathbf{x}_2^T [\mathbf{B}(t) \mathbf{u} + \mathbf{u}_b \\ &\quad - \mathbf{C}(\mathbf{p}, \dot{\mathbf{p}}) (\mathbf{x}_2 + \mathbf{v}) - \mathbf{G}(\mathbf{p}) - \mathbf{M}(\mathbf{p}) \dot{\mathbf{v}}] \\ &= \dot{V}_1 + \frac{1}{2} \mathbf{x}_2^T (\dot{\mathbf{M}}(\mathbf{p}) - 2\mathbf{C}(\mathbf{p}, \dot{\mathbf{p}})) \mathbf{x}_2 \\ &\quad + \mathbf{x}_2^T (\mathbf{B}(t) \mathbf{u} + \mathbf{u}_b - \mathbf{C}(\mathbf{p}, \dot{\mathbf{p}}) \mathbf{v} - \mathbf{G}(\mathbf{p}) - \mathbf{M}(\mathbf{p}) \dot{\mathbf{v}}) \end{aligned} \quad (20)$$

According to *Property 1*, (20) is simplified as

$$\dot{V}_2 = \dot{V}_1 + \mathbf{x}_2^T (\mathbf{B}(t) \mathbf{u} + \mathbf{u}_b - \mathbf{C}(\mathbf{p}, \dot{\mathbf{p}}) \mathbf{v} - \mathbf{G}(\mathbf{p}) - \mathbf{M}(\mathbf{p}) \dot{\mathbf{v}}) \quad (21)$$

According to *Properties 2 4*, we can obtain that

$$\begin{aligned} &\|\mathbf{C}(\mathbf{p}, \dot{\mathbf{p}}) \mathbf{v} + \mathbf{G}(\mathbf{p}) + \mathbf{M}(\mathbf{p}) \dot{\mathbf{v}}\| \\ &\leq \|\mathbf{C}(\mathbf{p}, \dot{\mathbf{p}}) \mathbf{v}\| + \|\mathbf{G}(\mathbf{p})\| + \|\mathbf{M}(\mathbf{p}) \dot{\mathbf{v}}\| \\ &\leq \underline{b} \left(\frac{\bar{c}}{\underline{b}} \|\dot{\mathbf{p}}\| \|\mathbf{v}\| + \frac{\bar{g}}{\underline{b}} + \frac{\bar{m}}{\underline{b}} \|\dot{\mathbf{v}}\| \right) \end{aligned} \quad (22)$$

Owing to the fact that the additive actuator fault \mathbf{u}_b is bounded, thus, there exists an unknown constant $\bar{u}_b > 0$ making the following inequality hold

$$\|\mathbf{u}_b\| \leq \bar{u}_b = \frac{b\bar{u}_b}{b} \quad (23)$$

Then, define the following two constants $\mu_1, \mu_2 > 0$:

$$\mu_1 = \max \left\{ \frac{\bar{c}}{\underline{b}}, \frac{\bar{g}}{\underline{b}}, \frac{\bar{m}}{\underline{b}} \right\}, \quad \mu_2 := \frac{\bar{u}_b}{\underline{b}} \quad (24)$$

It is obvious that the above two defined constants are bounded. By defining $\theta = \|\dot{p}\| \|\mathbf{v}\| + \|\dot{\mathbf{v}}\| + 1 > 0$, (22) becomes

$$\begin{aligned} & \|\mathbf{C}(\mathbf{p}, \dot{\mathbf{p}}) \mathbf{v} + \mathbf{G}(\mathbf{p}) + \mathbf{M}(\mathbf{p}) \dot{\mathbf{v}}\| \\ & \leq \underline{b} \left(\frac{\bar{c}}{\underline{b}} \|\dot{p}\| \|\mathbf{v}\| + \frac{\bar{g}}{\underline{b}} + \frac{\bar{m}}{\underline{b}} \|\dot{\mathbf{v}}\| \right) \\ & \leq \underline{b} \mu_1 \theta \end{aligned} \quad (25)$$

(23) becomes

$$\|\mathbf{u}_b\| \leq \underline{b} \mu_2 \quad (26)$$

Substituting (25) and (26) into (21) yields

$$\dot{V}_2 \leq \dot{V}_1 + \mathbf{x}_2^T \mathbf{B}(t) \mathbf{u} + (\underline{b} \mu_1 \theta + \underline{b} \mu_2) \|\mathbf{x}_2\| \quad (27)$$

According to the foregoing design procedure, the adaptive fault-tolerant controller is devised as

$$\mathbf{u} = -\mathbf{K}_2 \mathbf{x}_2 - \frac{1}{4\underline{b}} \mathbf{x}_2 - \frac{\hat{\mu}_1 \theta^2 \mathbf{x}_2}{\theta \|\mathbf{x}_2\| + \sigma_0} - \frac{\hat{\mu}_2 \mathbf{x}_2}{\|\mathbf{x}_2\| + \sigma_0} \quad (28)$$

where $\mathbf{K}_2 = \text{diag}\{K_{2,1}, \dots, K_{2,n}\} \in \mathbb{R}^{n \times n}$ is the positive-definite control gain. σ_0 is a positive constant. $\hat{\mu}_1, \hat{\mu}_2$ are the estimated values of unknown parameters μ_1, μ_2 . The relevant adaptive schemes are designed as

$$\begin{cases} \dot{\hat{\mu}}_1 = -\hat{\mu}_1 + \frac{\theta^2 \mathbf{x}_2^T \mathbf{x}_2}{\theta \|\mathbf{x}_2\| + \sigma_0} \\ \dot{\hat{\mu}}_2 = -\hat{\mu}_2 + \frac{\mathbf{x}_2^T \mathbf{x}_2}{\|\mathbf{x}_2\| + \sigma_0} \end{cases} \quad (29)$$

It is worth noting that function $\theta = \|\dot{p}\| \|\mathbf{v}\| + \|\dot{\mathbf{v}}\| + 1$ requires to calculate the derivative of virtual controller \mathbf{v} . However, as (15) presents, the form of \mathbf{v} is tedious. Namely, the derivative of \mathbf{v} is also very complex. To solve this problem, we use a linear tracking differentiator to estimate it. The corresponding tracking differentiator is expressed by

$$\begin{cases} \dot{z}_{1,i} = z_{2,i} \\ \dot{z}_{2,i} = -c_0^2 [c_1 (z_{1,i} - v_i) + c_2 z_{2,i}/c_0] \end{cases} \quad (i = 1, \dots, n) \quad (30)$$

where $z_{1,i}, z_{2,i} \in \mathbb{R}$ is the states of the tracking differentiator. c_0, c_1, c_2 are the relevant positive constants. Based on (30), the i th dimensional element of $\dot{\mathbf{v}}$ is approximated by $z_{2,i}$. The convergence of the tracking differentiator is proved by the following lemma.

Lemma 1. ([37]) For the linear tracking differentiator in (30), if c_0, c_1, c_2 are positive and $v_i(0), \dot{v}_i(0)$ are

bounded, then the estimated error $e_{v,i}(t) = z_{2,i}(t) - \dot{v}_i(t)$ is always bounded and the following equation holds

$$\lim_{t \rightarrow +\infty} e_{v,i}(t) = 0 \quad (31)$$

The detailed proof of Lemma 1 can be found in [37], which is omitted for brief. Based on the aforementioned discussions, one can use the state $z_{2,i}$ to approximate the \dot{v}_i to lower the computational complexity.

B. STABILITY ANALYSIS

According to the adaptive fault-tolerant controller design, one of important result is obtained in the following theorem.

Theorem 1: Under the devised controller and adaptive scheme in (28) and (29), the prescribed position tracking performance in (4) can be achieved in the whole time domain. Meanwhile, all the system signals involved in the close-loop tracking error system for system (1) are uniformly ultimately bounded in spite of unknown actuator faults.

Proof: The proof of Theorem 1 is organized as follows. First, construct the following Lyapunov function:

$$V_3 = V_2 + \frac{b}{2} (\tilde{\mu}_1^2 + \tilde{\mu}_2^2) \quad (32)$$

where $\tilde{\mu}_1, \tilde{\mu}_2$ are the estimation errors for unknown constants μ_1, μ_2 , respectively. Namely, they are defined as

$$\tilde{\mu}_1 = \mu_1 - \hat{\mu}_1, \quad \tilde{\mu}_2 = \mu_2 - \hat{\mu}_2 \quad (33)$$

Taking the derivative of V_3 yields

$$\dot{V}_3 = \dot{V}_2 + \underline{b} \tilde{\mu}_1 \dot{\tilde{\mu}}_1 + \underline{b} \tilde{\mu}_2 \dot{\tilde{\mu}}_2 \quad (34)$$

Substituting (16) and (27) into (34) gets

$$\begin{aligned} \dot{V}_3 &= \dot{V}_1 + \mathbf{x}_2^T \mathbf{B}(t) \mathbf{u} + (\underline{b} \mu_1 \theta + \underline{b} \mu_2) \|\mathbf{x}_2\| + \tilde{\mu}_1 \dot{\tilde{\mu}}_1 + \underline{b} \tilde{\mu}_2 \dot{\tilde{\mu}}_2 \\ &\leq -\sum_{i=1}^n \frac{K_{1,i} x_{1,i}^2}{(1 - x_{1,i}^2)^2} + \frac{1}{4} \sum_{i=1}^n x_{2,i}^2 + \mathbf{x}_2^T \mathbf{B}(t) \mathbf{u} \\ &\quad + (\underline{b} \mu_1 \theta + \underline{b} \mu_2) \|\mathbf{x}_2\| + \underline{b} \tilde{\mu}_1 \dot{\tilde{\mu}}_1 + \underline{b} \tilde{\mu}_2 \dot{\tilde{\mu}}_2 \end{aligned} \quad (35)$$

Substituting (28) into (35) yields

$$\begin{aligned} \dot{V}_3 &= \dot{V}_1 + \mathbf{x}_2^T \mathbf{B}(t) \mathbf{u} + (\underline{b} \mu_1 \theta + \underline{b} \mu_2) \|\mathbf{x}_2\| + \tilde{\mu}_1 \dot{\tilde{\mu}}_1 + \underline{b} \tilde{\mu}_2 \dot{\tilde{\mu}}_2 \\ &\leq -\sum_{i=1}^n \frac{K_{1,i} x_{1,i}^2}{(1 - x_{1,i}^2)^2} + \frac{1}{4} \sum_{i=1}^n x_{2,i}^2 - \mathbf{x}_2^T \mathbf{B}(t) \mathbf{K}_2 \mathbf{x}_2 \\ &\quad - \frac{1}{4\underline{b}} \mathbf{x}_2^T \mathbf{B}(t) \mathbf{x}_2 - \frac{\hat{\mu}_1 \theta^2 \mathbf{x}_2^T \mathbf{B}(t) \mathbf{x}_2}{\theta \|\mathbf{x}_2\| + \sigma_0} - \frac{\hat{\mu}_2 \mathbf{x}_2^T \mathbf{B}(t) \mathbf{x}_2}{\|\mathbf{x}_2\| + \sigma_0} \\ &\quad + (\underline{b} \mu_1 \theta + \underline{b} \mu_2) \|\mathbf{x}_2\| + \underline{b} \tilde{\mu}_1 \dot{\tilde{\mu}}_1 + \underline{b} \tilde{\mu}_2 \dot{\tilde{\mu}}_2 \end{aligned} \quad (36)$$

With consideration of $\|\mathbf{B}(t)\| \leq \underline{b}$, the following results can be obtained.

$$\begin{aligned} \frac{1}{4} \sum_{i=1}^n x_{2,i}^2 - \frac{1}{4\underline{b}} \mathbf{x}_2^T \mathbf{B}(t) \mathbf{x}_2 &\leq \frac{1}{4} \mathbf{x}_2^T \mathbf{x}_2 - \frac{1}{4} \mathbf{x}_2^T \mathbf{x}_2 = 0 \\ -\frac{\hat{\mu}_1 \theta^2 \mathbf{x}_2^T \mathbf{B}(t) \mathbf{x}_2}{\theta \|\mathbf{x}_2\| + \sigma_0} &\leq -\frac{\underline{b} \hat{\mu}_1 \theta^2 \mathbf{x}_2^T \mathbf{x}_2}{\theta \|\mathbf{x}_2\| + \sigma_0} \end{aligned}$$

$$-\frac{\hat{\mu}_2 \mathbf{x}_2^T \mathbf{B}(t) \mathbf{x}_2}{\|\mathbf{x}_2\| + \sigma_0} \leq -\frac{b \hat{\mu}_2 \mathbf{x}_2^T \mathbf{x}_2}{\|\mathbf{x}_2\| + \sigma_0} \quad (37)$$

Based on (37), (36) can be simplified as

$$\begin{aligned} \dot{V}_3 &\leq -\sum_{i=1}^n \frac{K_{1,i} x_{1,i}^2}{(1-x_{1,i}^2)^2} - \underline{b} \mathbf{x}_2^T \mathbf{K}_2 \mathbf{x}_2 + \underline{b} \tilde{\mu}_1 \dot{\mu}_1 + \underline{b} \tilde{\mu}_2 \dot{\mu}_2 \\ &\quad + \left(\underline{b} \mu_1 \theta \|\mathbf{x}_2\| - \frac{b \hat{\mu}_1 \theta^2 \mathbf{x}_2^T \mathbf{x}_2}{\theta \|\mathbf{x}_2\| + \sigma_0} \right) \\ &\quad + \left(\underline{b} \mu_2 \|\mathbf{x}_2\| - \frac{b \hat{\mu}_2 \mathbf{x}_2^T \mathbf{x}_2}{\|\mathbf{x}_2\| + \sigma_0} \right) \\ &\leq -\sum_{i=1}^n \frac{K_{1,i} x_{1,i}^2}{(1-x_{1,i}^2)^2} - \underline{b} \mathbf{x}_2^T \mathbf{K}_2 \mathbf{x}_2 + \underline{b} \tilde{\mu}_1 \dot{\mu}_1 + \underline{b} \tilde{\mu}_2 \dot{\mu}_2 \\ &\quad + \frac{b(\mu_1 - \hat{\mu}_1) \theta^2 \|\mathbf{x}_2\|^2}{\theta \|\mathbf{x}_2\| + \sigma_0} + \frac{b(\mu_2 - \hat{\mu}_2) \|\mathbf{x}_2\|^2}{\|\mathbf{x}_2\| + \sigma_0} \\ &\quad + \frac{\sigma_0 \underline{b} \mu_1 \theta \|\mathbf{x}_2\|}{\theta \|\mathbf{x}_2\| + \sigma_0} + \frac{b \sigma_0 \mu_2 \|\mathbf{x}_2\|}{\|\mathbf{x}_2\| + \sigma_0} \end{aligned} \quad (38)$$

With consideration of $\tilde{\mu}_1 = \mu_1 - \hat{\mu}_1$, $\tilde{\mu}_2 = \mu_2 - \hat{\mu}_2$, we can obtain $\dot{\tilde{\mu}}_1 = -\dot{\hat{\mu}}_1$, $\dot{\tilde{\mu}}_2 = -\dot{\hat{\mu}}_2$ due to the fact that μ_1 , μ_2 are constants. By substituting (29) into (38), the following inequality can be obtained

$$\begin{aligned} \dot{V}_3 &\leq -\sum_{i=1}^n \frac{K_{1,i} x_{1,i}^2}{(1-x_{1,i}^2)^2} - \underline{b} \mathbf{x}_2^T \mathbf{K}_2 \mathbf{x}_2 - \underline{b} \tilde{\mu}_1 \dot{\mu}_1 - \underline{b} \tilde{\mu}_2 \dot{\mu}_2 \\ &\quad + \frac{b \tilde{\mu}_1 \theta^2 \|\mathbf{x}_2\|^2}{\theta \|\mathbf{x}_2\| + \sigma_0} + \frac{b \tilde{\mu}_2 \|\mathbf{x}_2\|^2}{\|\mathbf{x}_2\| + \sigma_0} \\ &\quad + \frac{b \sigma_0 \mu_1 \theta \|\mathbf{x}_2\|}{\theta \|\mathbf{x}_2\| + \sigma_0} + \frac{b \sigma_0 \mu_2 \|\mathbf{x}_2\|}{\|\mathbf{x}_2\| + \sigma_0} \\ &\leq -\sum_{i=1}^n \frac{K_{1,i} x_{1,i}^2}{(1-x_{1,i}^2)^2} - \underline{b} \mathbf{x}_2^T \mathbf{K}_2 \mathbf{x}_2 + \underline{b} \tilde{\mu}_1 \dot{\mu}_1 + \underline{b} \tilde{\mu}_2 \dot{\mu}_2 \\ &\quad + \frac{b \sigma_0 \mu_1 \theta \|\mathbf{x}_2\|}{\theta \|\mathbf{x}_2\| + \sigma_0} + \frac{b \sigma_0 \mu_2 \|\mathbf{x}_2\|}{\|\mathbf{x}_2\| + \sigma_0} \end{aligned} \quad (39)$$

For (39), the following result is obtained

$$\begin{aligned} \frac{b \sigma_0 \mu_1 \theta \|\mathbf{x}_2\|}{\theta \|\mathbf{x}_2\| + \sigma_0} + \frac{b \sigma_0 \mu_2 \|\mathbf{x}_2\|}{\|\mathbf{x}_2\| + \sigma_0} &\leq \sigma_0 \underline{b} \mu_1 + \sigma_0 \underline{b} \mu_2 \\ &= \sigma_0 \underline{b} (\mu_1 + \mu_2) \end{aligned} \quad (40)$$

Based on (40), (39) is further simplified as

$$\begin{aligned} \dot{V}_3 &\leq -\sum_{i=1}^n \frac{K_{1,i} x_{1,i}^2}{(1-x_{1,i}^2)^2} - \underline{b} \mathbf{x}_2^T \mathbf{K}_2 \mathbf{x}_2 + \underline{b} \tilde{\mu}_1 (\mu_1 - \tilde{\mu}_1) \\ &\quad + \underline{b} \tilde{\mu}_2 (\mu_2 - \tilde{\mu}_2) + \sigma_0 \underline{b} (\mu_1 + \mu_2) \\ &= -\sum_{i=1}^n \frac{K_{1,i} x_{1,i}^2}{(1-x_{1,i}^2)^2} - \underline{b} \mathbf{x}_2^T \mathbf{K}_2 \mathbf{x}_2 - \underline{b} \tilde{\mu}_1^2 - \underline{b} \tilde{\mu}_2^2 \\ &\quad + \underline{b} \tilde{\mu}_1 \mu_1 + \underline{b} \tilde{\mu}_2 \mu_2 + \sigma_0 \underline{b} (\mu_1 + \mu_2) \end{aligned} \quad (41)$$

By applying Young's inequality, we can obtain

$$\begin{cases} \underline{b} \tilde{\mu}_1 \mu_1 \leq \frac{b}{2} \tilde{\mu}_1^2 + \frac{b}{2} \mu_1^2 \\ \underline{b} \tilde{\mu}_2 \mu_2 \leq \frac{b}{2} \tilde{\mu}_2^2 + \frac{b}{2} \mu_2^2 \end{cases} \quad (42)$$

Accordingly, (41) becomes

$$\begin{aligned} \dot{V}_3 &\leq -\sum_{i=1}^n \frac{K_{1,i} x_{1,i}^2}{(1-x_{1,i}^2)^2} - \underline{b} \mathbf{x}_2^T \mathbf{K}_2 \mathbf{x}_2 - \frac{b}{2} \tilde{\mu}_1^2 - \frac{b}{2} \tilde{\mu}_2^2 \\ &\quad + \frac{b}{2} \mu_1^2 + \frac{b}{2} \mu_2^2 + \sigma_0 (\mu_1 + \mu_2) \end{aligned} \quad (43)$$

Define the following two constants $\lambda_1, \lambda_2 > 0$

$$\begin{cases} \lambda_1 = \min \left\{ \min_i 2K_{1,i}, 2\underline{b} \min_i K_{2,i}/\bar{m}, 1 \right\} \\ \lambda_2 = \frac{b}{2} \mu_1^2 + \frac{b}{2} \mu_2^2 + \sigma_0 \underline{b} (\mu_1 + \mu_2) \end{cases} \quad (44)$$

Thus, (43) becomes

$$\dot{V}_3 \leq -\lambda_1 V_3 + \lambda_2 \quad (45)$$

Based on the above equation, we can obtain that all the signals involved in the close-loop tracking error system are uniformly ultimately bounded. In the meanwhile, the following conclusion can be obtained

$$\frac{1}{2} \frac{x_{1,i}^2(t)}{1-x_{1,i}^2(t)} \leq V_1(t) \leq V_3(t) \leq \delta \quad (i=1, \dots, n) \quad (46)$$

where δ is a positive constant. Based on (46), we can obtain

$$|x_{1,i}(t)| \leq \sqrt{\frac{2\delta}{2\delta+1}} \quad (i=1, \dots, n) \quad (47)$$

Due to $x_{1,i}(t) = p_{e,i}(t)/\alpha_i(t)$, we can obtain

$$|p_{e,i}(t)| \leq \sqrt{\frac{2\delta}{2\delta+1}} \alpha_i(t) < \alpha_i(t) \quad (i=1, \dots, n) \quad (48)$$

As presented in (48), we can find that the prescribed tracking performance can be achieved in the whole time domain. Accordingly, the proof of Theorem 1 is finished. ■

IV. APPLICATION TO A 2-LINK ROBOTIC MANIPULATOR

A. DYNAMIC DESCRIPTION OF A 2-LINK ROBOTIC MANIPULATOR

To demonstrate the effectiveness of the proposed control method, in this part, a 2-link robotic manipulator works as the simulation object, which is illustrated in Fig. 1.

As shown in Fig. 1, m_1, m_2, l_1, l_2 denote the mass and length of the two links, respectively. $p = [p_1, p_2]^T$, $\dot{p} = [\dot{p}_1, \dot{p}_2]^T \in \mathbb{R}^2$ is the joint angles and angle velocity of the 2-link manipulator, respectively. The dynamics of the manipulator are expressed by [35] the equation can be derived, as shown at the bottom of next page wherein, g is the gravitational acceleration in the foregoing matrices.

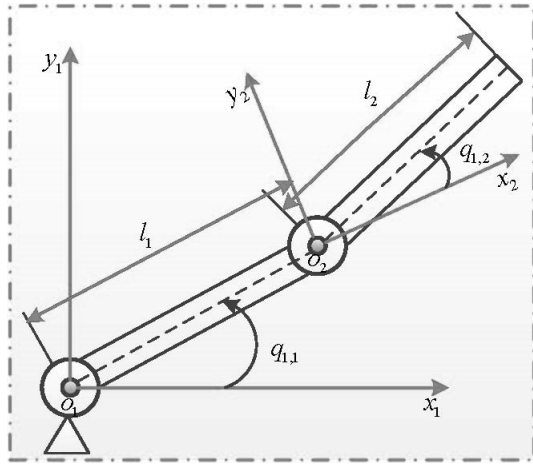


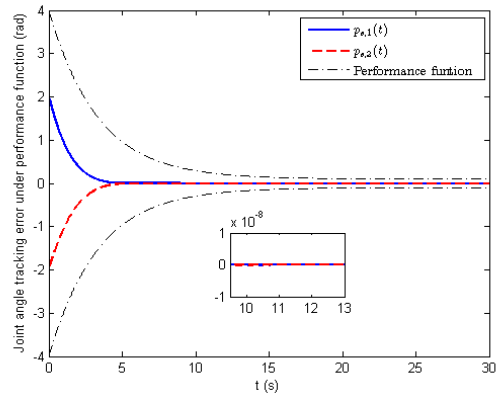
FIGURE 1. Geometric representation of the 2-link robotic manipulator.

B. STABILIZATION CONTROL OF JOINT ANGLE FOR THE 2-LINK ROBOTIC MANIPULATOR

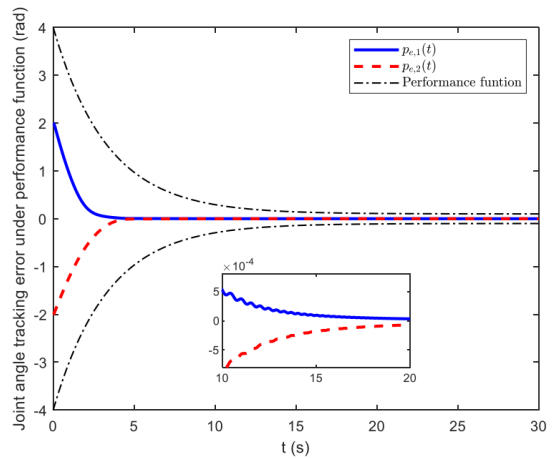
Based on the foregoing dynamic description, in this part, the joint angle stabilization control is organized. The desired reference command is $p_d(t) = [p_{d,1}(t), p_{d,2}(t)]^T = [0, 0]^T rad$. The simulation parameters are chosen as: $m_1 = 0.5 kg, m_2 = 1.5 kg, l_1 = 1.0 m, l_2 = 0.8 m. g = 9.8 m/s^2, \alpha_{i,0} = 4, \alpha_{i,\infty} = 0.1, \gamma_i = 0.3, \mathbf{K}_1 = diag\{0.1, 0.1\}, \mathbf{K}_2 = diag\{100, 100\}, \sigma_0 = 0.001$. The initial simulation conditions are set as $p(0) = [p_1(0), p_2(0)]^T = [2, -2]^T rad, \hat{\mu}_1(0) = \hat{\mu}_2(0) = 1, \dot{p}(0) = [\dot{p}_1(0), \dot{p}_2(0)]^T = [0, 0] rad/s$. To further validate the robustness of the proposed control scheme, the LuGre joint friction model, as a universal one in the robotic systems, is applied to describe a typical type of external disturbance or noise in the control input, which is expressed by

$$\begin{cases} \tau_{d,i} = -\chi_{0,i}w_i - \chi_{1,i}\dot{w}_i - \chi_{2,i}\dot{p}_i \\ \dot{w}_i = \dot{p}_i - \chi_{0,i}| \dot{p}_i | w_i / \varrho_i (\dot{p}_i) \\ \varrho_i(\dot{p}_i) = F_{c,i} + (F_{s,i} - F_{c,i}) \exp(-|\dot{p}_i| / \dot{p}_{s,i}) \end{cases} \quad (49)$$

where $\chi_{0,i}, \chi_{1,i}, \chi_{2,i}$ ($i = 1, 2$) denote the stiffness parameter, the damping parameter and the viscous friction parameter, respectively. w_i, ϱ_i are the intermediate variables. $F_{c,i}, F_{s,i}$ are, respectively, the Coulomb friction parameter and static friction term. $\dot{p}_{s,i} > 0$ is the joint stibeck velocity. According to [38], the above parameters are selected as $\chi_{0,i} = 280, \chi_{1,i} = 1, \chi_{2,i} = 0.017, F_{c,i} = 0.22, F_{s,i} = 0.39, \dot{p}_{s,i} = 0.1$ ($i = 1, 2$). To show the effectiveness of the proposed



(a) with the proposed control scheme



(b) with the proposed control scheme in [38]

FIGURE 2. Time response of joint angle without actuator faults.

control scheme, the simulation results under the proposed controller in [38] are as the comparative test. In this part, two cases are considered.

1) STABILIZATION CONTROL WITHOUT ACTUATOR FAULTS

When there are no actuator faults, $\mathbf{B}(t) = diag\{1, 1\}, \mathbf{u}_b = [0, 0]^T, \underline{b} = 1$, then, the corresponding simulation results are shown in Figs. 2-5.

As shown in Figs. 2-5, one can conclude that: The joint angle of the 2-link robotic manipulator can be stabilized around 5 seconds under the two control schemes (see Figs. 2 and 3). However, Fig. 2 demonstrates that the ultimate tracking accuracy is improved dramatically with the proposed control scheme. Meanwhile, the control torques of the robotic

$$\begin{aligned} \mathbf{M}(p) &= \begin{bmatrix} (m_1 + m_2)l_1^2 + m_2l_2^2 + 2m_2l_1l_2 \cos(p_2) & m_2(l_2^2 + l_1l_2 \cos(p_2)) \\ m_2(l_2^2 + l_1l_2 \cos(p_2)) & m_2l_2^2 \end{bmatrix} \\ \mathbf{C}(p, \dot{p}) &= \begin{bmatrix} -m_2l_1l_2 \sin(p_2)\dot{p}_2 & -m_2l_1l_2 \sin(p_2)\dot{p}_2 - m_2l_1l_2 \sin(p_2)\dot{p}_1 \\ m_2l_1l_2 \sin(p_2)\dot{p}_1 & 0 \end{bmatrix} \\ \mathbf{G}(p) &= \begin{bmatrix} (m_1 + m_2)gl_1 \sin(p_1) + m_2gl_2 \sin(p_1 + p_2) \\ m_2gl_2 \sin(p_1 + p_2) \end{bmatrix} \end{aligned}$$

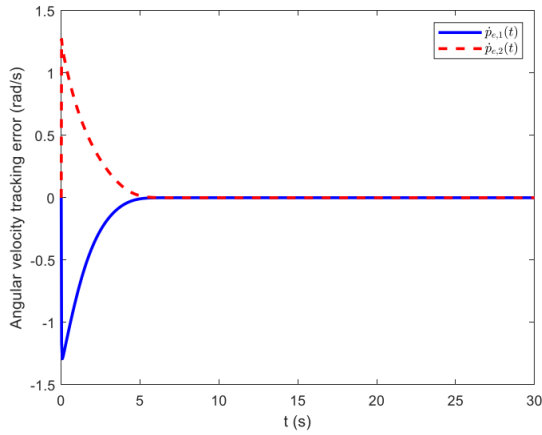


FIGURE 3. Time response of joint angle velocity without actuator faults.

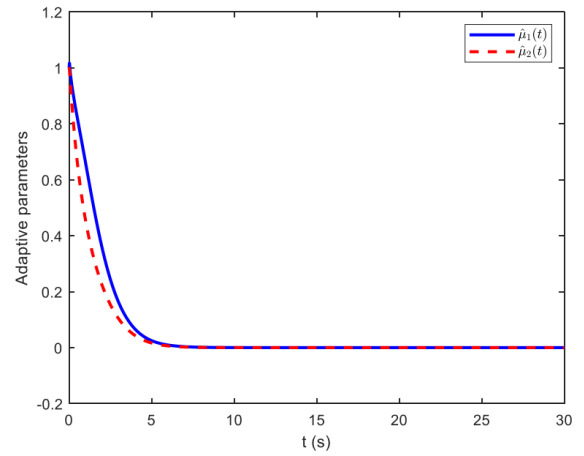
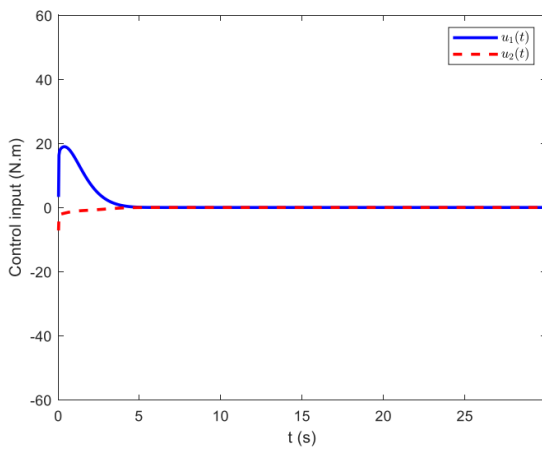
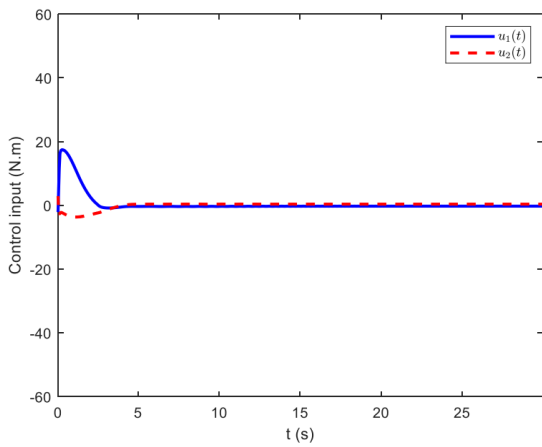


FIGURE 5. Time response of adaptive parameters without actuator faults.

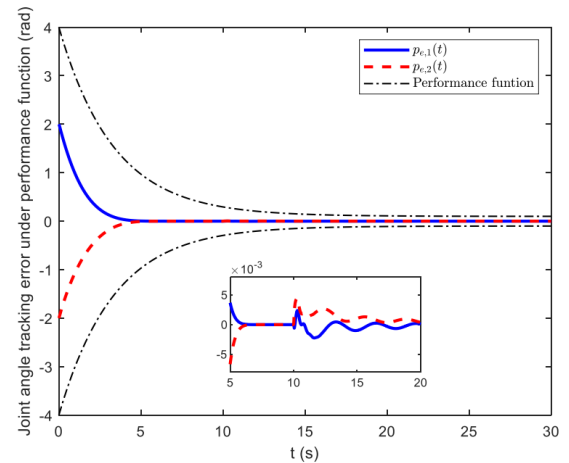


(a) with the proposed control scheme

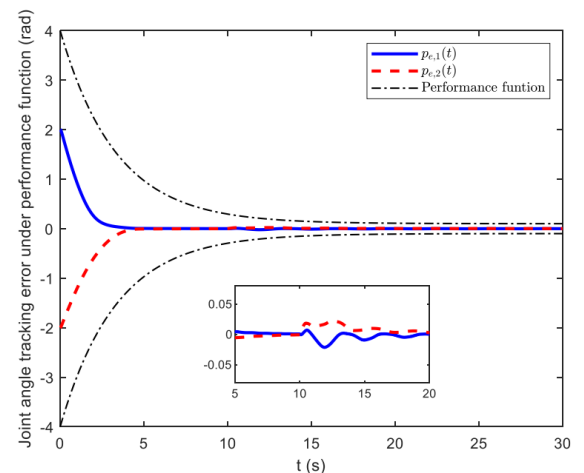


(b) with the proposed control scheme in [38]

FIGURE 4. Control torques of the 2-link robotic manipulator without actuator faults.



(a) with the proposed control scheme



(b) with the proposed control scheme in [38]

FIGURE 6. Time response of joint angle with actuator faults.

manipulator are bounded. Figure 5 shows that the adaptive parameters are convergent under the designed adaptive scheme. To be brief, the joint angle of the 2-link robotic manipulator can be stabilized quickly under the two control schemes without actuator faults.

2) STABILIZATION CONTROL WITH ACTUATOR FAULTS

To further validate the effectiveness of the proposed control method, stabilization control with actuator faults is

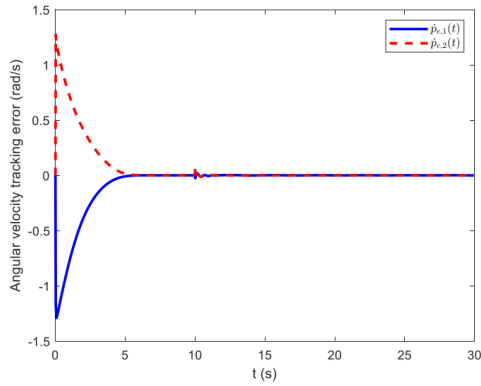


FIGURE 7. Time response of joint angle velocity with actuator faults.

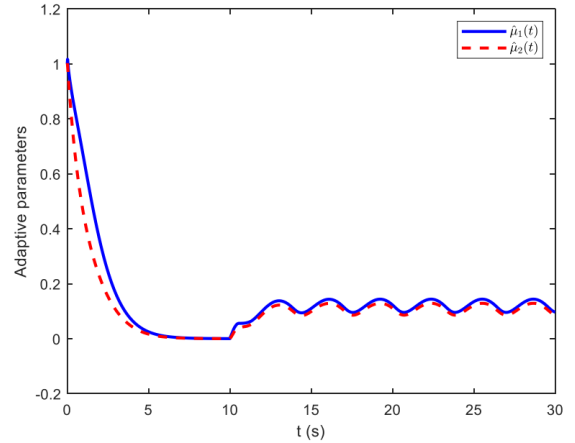
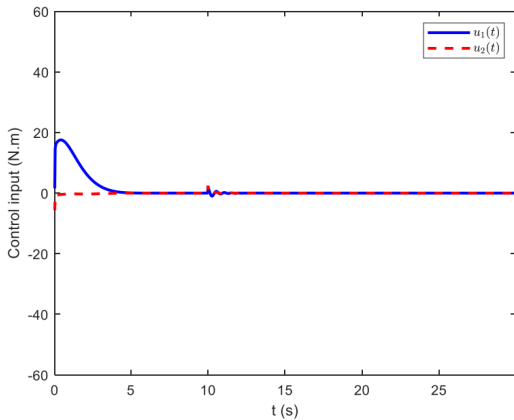
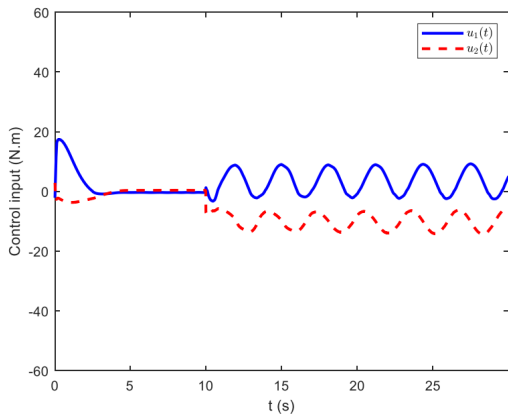


FIGURE 9. Time response of adaptive parameters with actuator faults.



(a) with the proposed control scheme

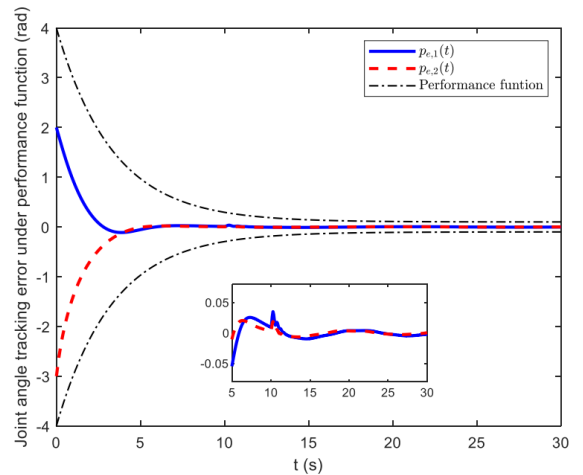


(b) with the proposed control scheme in [38]

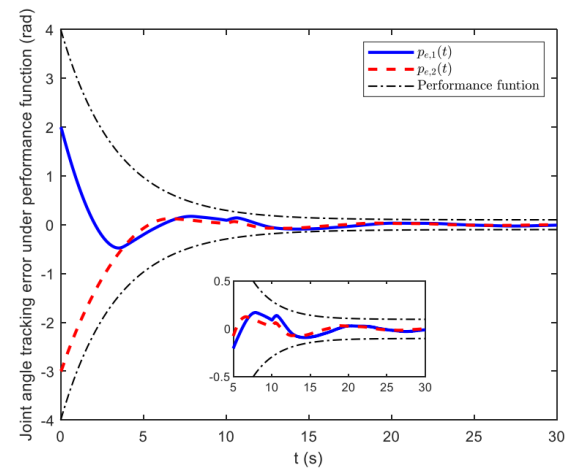
FIGURE 8. Control torques of the 2-link robotic manipulator with actuator faults.

organized. The relevant actuator fault model is expressed by

$$\begin{cases} \mathbf{B}(t) = \begin{cases} \text{diag}\{1, 1\}, & t < 10 \\ \text{diag}\{0.3, 0.2\}, & t \geq 10 \end{cases} \\ \mathbf{u}_b = \begin{cases} 2 \sin(t) - 1, & t < 10 \\ \cos(t) + 2, & t \geq 10 \end{cases} \\ \underline{b} = \begin{cases} 1, & t < 10 \\ 0.1, & t \geq 10 \end{cases} \end{cases} \quad (50)$$



(a) with the proposed control scheme



(b) with the proposed control scheme in [38]

FIGURE 10. Time response of joint angle tracking error with actuator faults.

The relevant simulation parameters keep the same. Then, the corresponding simulation results are shown in Figs. 6-9.

As shown in Figs. 6-9, one can conclude that: Under the two control schemes, the joint angle of the 2-link robotic

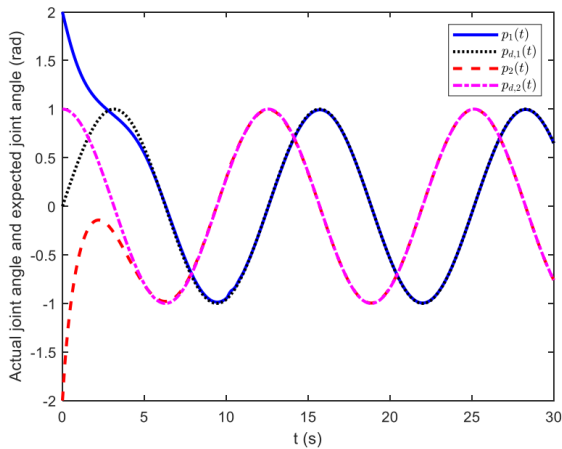


FIGURE 11. Tracking trajectory of joint angle velocity with actuator faults.

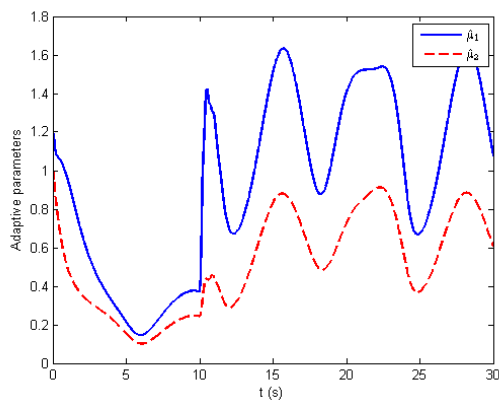


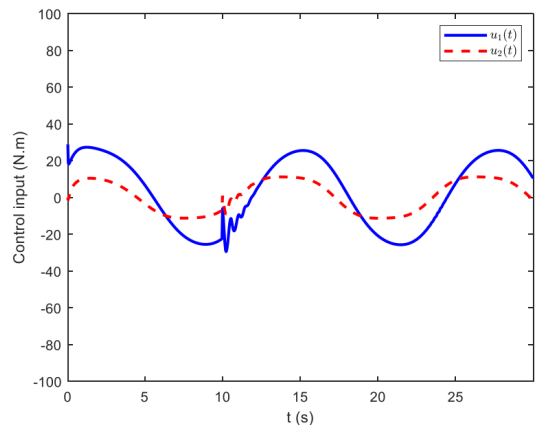
FIGURE 12. Time response of adaptive parameters in the angle tracking.

manipulator can be stabilized around 5 seconds before the actuator faults appear (see Figs. 6 and 7). When the actuator faults appear at 10 seconds, there exists a chattering phenomenon in the states and control input. This chattering phenomenon only lasts for about 1 second under the proposed control scheme. However, the chattering phenomenon lasts for a long time after 10 seconds under the control scheme in [38], which leads to much more fuel consumptions compared with the proposed control scheme. This is because that, in this work, the adaptive parameters change actively to compensate for the negative effects induced by the actuator faults as Fig. 9 presents. Thus, in spite of the actuator faults, the joint angle of the 2-link robotic manipulator can be also stabilized in the proposed control scheme with higher tracking accuracy. So, the devised controller and adaptive scheme are effective.

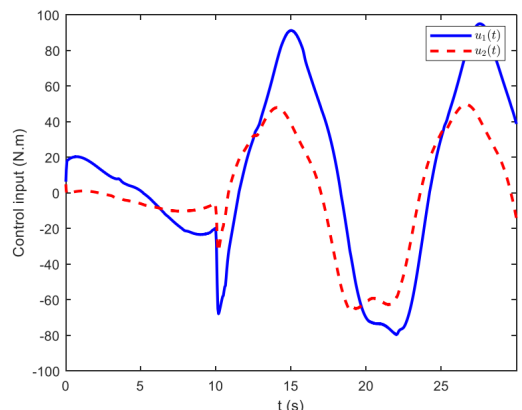
C. TRACKING CONTROL OF JOINT ANGLE FOR THE 2-LINK ROBOTIC MANIPULATOR

In this part, the joint angle tracking control of the 2-link robotic manipulator is organized to further validate the effectiveness of the proposed control method. Without loss of generality, the desired reference command is chosen as:

$$p_d(t) = [p_{d,1}(t), p_{d,2}(t)]^T = \begin{bmatrix} \sin(0.5t) \\ \cos(0.5t) \end{bmatrix} rad \quad (51)$$



(a) with the proposed control scheme



(b) with the proposed control scheme in [38]

FIGURE 13. Control torques of the 2-link robotic manipulator in the angle tracking.

The simulation parameters and actuator fault model are the same as those in subsection 4.2.2. Then, the corresponding simulation results are shown in Figs. 10-13.

As shown in Figs. 10-13, one can conclude that: Figures 10 and 11 show that the desired reference command can be tracked around 7 seconds. When the actuator faults appear at 10 seconds, there is a chattering phenomenon in the states and control input. However, this chattering phenomenon will disappear and the relevant tracking accuracy is improved by one order of magnitude under the proposed control scheme compared with that in [38]. This can be explained that after 10 seconds, the adaptive parameters change actively to compensate for the negative effects brought by the actuator faults (see Fig. 12). Moreover, Fig. 13 illustrates that the control input of the proposed control scheme is very smaller than that in [38]. In this case, the fuel consumption is pretty smaller under the proposed control scheme.

Based on the aforementioned three groups of numerical simulation results, we can find that the proposed control method is effective to address the joint angle stabilization and tracking problem in spite of actuator faults.

V. CONCLUSION AND FUTURE WORK

The adaptive fault-tolerant guaranteed performance control method has been established for the Euler-Lagrange system

subject to uncertain actuator faults in this paper. Compared with the existing works, the prominent advantage of the proposed method is that the uncertain actuator faults are not required to identify online and the conventional logarithmic transformation is omitted in the controller design. Thus, the developed control scheme is easily achieved by the practical systems. Moreover, the simulation results on the joint angle stabilization and tracking demonstrate the effectiveness of the proposed control method.

In the future work, we may extend the proposed control method to solve the formation control problem of multiple EL systems with consideration of the limited communication ranges and burden. Moreover, the unmeasurable state problem as presented in [14], [15] also deserves investigations for the EL systems in the PPC structure.

DECLARATION OF COMPETING INTEREST

The authors declare no conflict of interest in preparing this article.

REFERENCES

- [1] S.-J. Chung and J.-J.-E. Slotine, "Cooperative robot control and concurrent synchronization of lagrangian systems," *IEEE Trans. Robot.*, vol. 25, no. 3, pp. 686–700, Jun. 2009.
- [2] P. M. Patre, W. MacKunis, M. Johnson, and W. E. Dixon, "Composite adaptive control for Euler–Lagrange systems with additive disturbances," *Automatica*, vol. 46, no. 1, pp. 140–147, Jan. 2010.
- [3] Y. Li, D. Zhao, Z. Zhang, and J. Liu, "An IDRA approach for modeling helicopter based on Lagrange dynamics," *Appl. Math. Comput.*, vol. 265, pp. 733–747, Aug. 2015.
- [4] M. Wang, Y. Chai, and J. Luo, "A novel prescribed performance controller with unknown dead-zone and impactive disturbance," *IEEE Access*, vol. 8, pp. 17160–17169, 2020.
- [5] B. Gong, S. Li, Y. Yang, J. Shi, and W. Li, "Maneuver-free approach to range-only initial relative orbit determination for spacecraft proximity operations," *Acta Astronautica*, vol. 163, pp. 87–95, Oct. 2019.
- [6] Y. Sun, D. Dong, H. Qin, N. Wang, and X. Li, "Distributed coordinated tracking control for multiple uncertain Euler–Lagrange systems with time-varying communication delays," *IEEE Access*, vol. 7, pp. 12598–12609, 2019.
- [7] N. Sharma, S. Bhasin, Q. Wang, and W. E. Dixon, "Predictor-based control for an uncertain Euler–Lagrange system with input delay," *Automatica*, vol. 47, no. 11, pp. 2332–2342, 2011.
- [8] X. Lai, Y. Wang, M. Wu, and W. Cao, "Stable control strategy for planar three-link underactuated mechanical system," *IEEE/ASME Trans. Mechatronics*, vol. 21, no. 2, pp. 1345–1356, Jun. 2016.
- [9] Z. Feng, J. Guo, and J. Zhou, "Robust constrained autopilot control for a generic missile in the presence of state and input constraints," *Optik*, vol. 149, pp. 49–58, Nov. 2017.
- [10] Q. Yang, H. Fang, J. Chen, Z.-P. Jiang, and M. Cao, "Distributed global output-feedback control for a class of Euler–Lagrange systems," *IEEE Trans. Autom. Control*, vol. 62, no. 9, pp. 4855–4861, Sep. 2017.
- [11] C. Li, L. Chen, Y. Guo, and G. Ma, "Formation–containment control for networked Euler–Lagrange systems with input saturation," *Nonlinear Dyn.*, vol. 91, no. 2, pp. 1307–1320, 2018.
- [12] Y. Sun, L. Chen, G. Ma, and C. Li, "Adaptive neural network tracking control for multiple uncertain Euler–Lagrange systems with communication delays," *J. Franklin Inst.*, vol. 354, no. 7, pp. 2677–2698, 2017.
- [13] A. Green and J. Z. Sasiadek, "Adaptive control of a flexible robot using fuzzy logic," *J. Guid., Control, Dyn.*, vol. 28, no. 1, pp. 36–42, Jan. 2005.
- [14] Y. Li, K. Sun, and S. Tong, "Observer-based adaptive fuzzy fault-tolerant optimal control for SISO nonlinear systems," *IEEE Trans. Cybern.*, vol. 49, no. 2, pp. 649–661, Feb. 2019.
- [15] S. Tong, K. Sun, and S. Sui, "Observer-based adaptive fuzzy decentralized optimal control design for strict-feedback nonlinear large-scale systems," *IEEE Trans. Fuzzy Syst.*, vol. 26, no. 2, pp. 569–584, Apr. 2018.
- [16] X. Mao, H. Zhang, and Y. Wang, "Flocking of quad-rotor UAVs with fuzzy control," *ISA Trans.*, vol. 74, pp. 185–193, Mar. 2018.
- [17] C. Wei, J. Luo, H. Dai, and J. Yuan, "Adaptive model-free constrained control of postcapture flexible spacecraft: A Euler–Lagrange approach," *J. Vib. Control*, vol. 24, no. 20, pp. 4885–4903, 2018.
- [18] S. J. Yoo, "Actuator fault detection and adaptive accommodation control of flexible-joint robots," *IET Control Theory Appl.*, vol. 6, no. 10, pp. 1497–1507, Jul. 2012.
- [19] Z. Gao, C. Cecati, and S. X. Ding, "A survey of fault diagnosis and fault-tolerant techniques—Part I: Fault diagnosis with model-based and signal-based approaches," *IEEE Trans. Ind. Electron.*, vol. 62, no. 6, pp. 3757–3767, Jun. 2015.
- [20] C. Wei, J. Luo, H. Dai, Z. Yin, and J. Yuan, "Low-complexity differentiator-based decentralized fault-tolerant control of uncertain large-scale nonlinear systems with unknown dead zone," *Nonlinear Dyn.*, vol. 89, no. 4, pp. 2573–2592, Sep. 2017.
- [21] L. Liu, Y.-J. Liu, D. Li, S. Tong, and Z. Wang, "Barrier Lyapunov function-based adaptive fuzzy FTC for switched systems and its applications to resistance–inductance–capacitance circuit system," *IEEE Trans. Cybern.*, vol. 50, no. 8, pp. 3491–3502, Aug. 2019.
- [22] S. Yin, B. Xiao, S. X. Ding, and D. Zhou, "A review on recent development of spacecraft attitude fault tolerant control system," *IEEE Trans. Ind. Electron.*, vol. 63, no. 5, pp. 3311–3320, May 2016.
- [23] C. Wei, Y. Liao, W. Xi, Z. Yin, and J. Luo, "Event-driven adaptive fault-tolerant tracking control for uncertain mechanical systems with application to flexible spacecraft," *J. Vib. Control*, vol. 26, nos. 19–20, pp. 1735–1752, 2020.
- [24] B. Gong, J. Luo, S. Li, and W. Li, "Observability criterion of angles-only navigation for spacecraft proximity operations," *Proc. Inst. Mech. Eng., G, J. Aerosp. Eng.*, vol. 233, no. 12, pp. 4302–4315, Sep. 2019.
- [25] C. P. Bechlioulis and G. A. Rovithakis, "Robust adaptive control of feedback linearizable MIMO nonlinear systems with prescribed performance," *IEEE Trans. Autom. Control*, vol. 53, no. 9, pp. 2090–2099, Oct. 2008.
- [26] C. Wei, J. Luo, H. Dai, and G. Duan, "Learning-based adaptive attitude control of spacecraft formation with guaranteed prescribed performance," *IEEE Trans. Cybern.*, vol. 49, no. 11, pp. 4004–4016, Nov. 2019.
- [27] Z. Yin, A. Suleman, J. Luo, and C. Wei, "Appointed-time prescribed performance attitude tracking control via double performance functions," *Aerosp. Sci. Technol.*, vol. 93, Oct. 2019, art. no. 105337.
- [28] A. K. Kostarigka and G. A. Rovithakis, "Prescribed performance output Feedback/Observer-free robust adaptive control of uncertain systems using neural networks," *IEEE Trans. Syst., Man, Cybern., B (Cybern.)*, vol. 41, no. 6, pp. 1483–1494, Dec. 2011.
- [29] K. Zhao, Y. Song, T. Ma, and L. He, "Prescribed performance control of uncertain Euler–Lagrange systems subject to full-state constraints," *IEEE Trans. Neural Netw. Learn. Syst.*, vol. 29, no. 8, pp. 3478–3489, Aug. 2018.
- [30] H. J. Asl, T. Narikiyo, and M. Kawanishi, "Bounded-input prescribed performance control of uncertain Euler–Lagrange systems," *IET Control Theory Appl.*, vol. 13, no. 1, pp. 17–26, 2019.
- [31] Y. Zhu, J. Qiao, and L. Guo, "Adaptive sliding mode disturbance observer-based composite control with prescribed performance of space manipulators for target capturing," *IEEE Trans. Ind. Electron.*, vol. 66, no. 3, pp. 1973–1983, Mar. 2019.
- [32] L. Tang, A. Chen, and D. Li, "Time-varying tan-type barrier Lyapunov function-based adaptive fuzzy control for switched systems with unknown dead zone," *IEEE Access*, vol. 7, pp. 110928–110935, 2019.
- [33] L. Liu, Y.-J. Liu, A. Chen, S. Tong, and C. L. P. Chen, "Integral barrier Lyapunov function-based adaptive control for switched nonlinear systems," *Sci. China Inf. Sci.*, vol. 63, no. 3, pp. 1–14, Mar. 2020.
- [34] F. Cunningham, Jr., and N. Grossman, "On young's inequality," *Amer. Math. Monthly*, vol. 78, no. 7, pp. 781–783, 1971.
- [35] Z. Yin, J. Luo, and C. Wei, "Quasi fixed-time fault-tolerant control for nonlinear mechanical systems with enhanced performance," *Appl. Math. Comput.*, vol. 352, pp. 157–173, Jul. 2019.
- [36] J. Lei, J. Yang, J. Zhao, and H. Wu, "Backstepping sliding mode lane keeping control of lateral position error with dynamic of tire steering device," *Optik*, vol. 127, no. 5, pp. 2439–2443, Mar. 2016.
- [37] X. Wang, Z. Chen, and Z. Yuan, "Design and analysis for new discrete tracking-differentiators," *Appl. Mathematics-A J. Chin. Universities*, vol. 18, no. 2, pp. 214–222, Jun. 2003.
- [38] Z. Yin, J. Luo, and C. Wei, "Robust prescribed performance control for Euler–Lagrange systems with practically finite-time stability," *Eur. J. Control*, vol. 52, pp. 1–10, Mar. 2020.



GANG ZHANG received the B.S. degree from the Yan Cheng Institute of Technology in 2008 and the M.S. degree from Dalian University in 2011. He is currently pursuing the Ph.D. degree with the China University of Mining and Technology. His research interests include nonlinear system control and prescribed performance control.



DEQIANG CHENG received the B.S., M.S., and Ph.D. degrees in electrical and information engineering from the China University of Mining and Technology. He is currently a Professor with the China University of Mining and Technology. His research interests include machine learning, video coding, image processing, pattern recognition, and nonlinear system control.

...